Synthesis and Characterization of the First Sandwich Complex of Trivalent Thorium: A Structural Comparison with the Uranium Analogue

Julian S. Parry,[†] F. Geoffrey N. Cloke,*[,†] Simon J. Coles,[‡] and Michael B. Hursthouse[‡]

Contribution from The Chemistry Laboratory, School of Chemistry, Physics and Environmental Science, University of Sussex, Brighton BN1 9QJ, UK, and EPSRC National Crystallography Service, Department of Chemistry, University of Southampton, Highfield, Southampton

Received February 5, 1999

Abstract: Reduction of the bulky 8-annulene thorium complex [Th{COT(TBS)$_2$}$_2$] (COT(TBS)$_2$ = η-C$_8$H$_6$(*t*BuMe$_2$-Si)$_2$-1,4) by potassium yields the anionic compound {Th[COT(TBS)$_2$]$_2$}K·(DME)$_2$, which was crystallographically characterized and is the first sandwich complex of Th(III). EPR spectroscopy indicates that the molecule possesses a 6d^1 ground state. A structural comparison is made with the isostructural uranium(III) complex and the thorium(IV) parent compound.

Introduction

Although bis(8-annulene)uranium, [U(COT)$_2$] (COT= η-C$_8$H$_8$), was first synthesized nearly 30 years ago,[1,2] and despite the fact that there are several trivalent early actinide complexes stabilized by the cyclopentadienyl anion and its derivatives,[3−5] the first structurally characterized trivalent early actinide 8-annulene sandwich complex was reported only as recently as 1991.[6−8] In contrast, trivalent lanthanide COT complexes such as {Ce(COT)$_2$}$^-$ are relatively common and anionic analogues containing the later actinides such as Np and Pu are also known.[9] In principle, there is no obvious reason for this discrepancy since COT sandwich complexes are highly symmetric and provide an ideal framework to attach sterically demanding functional groups. These are usually required to kinetically stabilize such large and generally highly reactive metal centers against the decomposition pathways that tend to plague them.[10,11] Nevertheless, a comparison has been drawn between the existence of the cerium(III) compound {Ce(COT)$_2$}$^-$ vs the nonexistence of the thorium(III) compound {Th(COT)$_2$}$^-$, where the discrepancy was ascribed to the preference for thorium over cerium and the lanthanides in general to exist in the +4 oxidation state.[12]

A molecular orbital (MO) diagram for An(COT)$_2$ (An = actinide) is shown in Figure 1.[13,14]The most conspicuous covalent interactions which are primarily responsible for the stability of these molecules involve the metal 6dδ and ligand group 3e$_{2g}$ orbitals and the metal 5fδ and 3e$_{2u}$ ligand group orbitals.[15] The antibonding counterpart of the latter consists mostly of metal 5fδ, so this orbital is destabilized with respect to its parent atomic orbital (AO). Conversely, the interaction of the 5fϕ orbitals with the high-lying ligand e$_{3u}$ antibonding orbitals stabilizes the former with respect to their parent AO's. The two remaining essentially nonbonding 5f orbitals, the fσ and fπ, lie between these two limits. Above the 5f series lies the 6dσ orbital, which is also essentially nonbonding due to poor overlap with the low-lying ligand A$_{1g}$ orbitals.[16] Placing one electron in the lowest lying 5f-based e$_{3u}$ orbital yields a qualitative diagram for {Th(COT)$_2$}$^-$. This hypothetical thorium(III) compound has the same electronic configuration as the known compound, Pa(COT)$_2$, and would be expected to generate an EPR signal only at low temperature rather like its U(V) 5f^1 analogue, {U(CHT)$_2$}$^-$ (CHT = cycloheptatrienyl trianion).[17−19] The trivalent compound becomes thermodynamically more stable than its tetravalent parent because the former can engage in metal-to-ligand ϕ-back-bonding to the empty ligand e$_{3u}$ orbitals.[13,20] Substituents on the COT rings such as trialkylsilyl groups would be expected to encourage this back-donation by lowering the energy of the e$_{3u}$ ligand orbitals.[21] The dashed line

[†] University of Sussex.
[‡] University of Southampton.

(1) Streitwieser, A., Jr.; Muller-Westerhoff, U. *J. Am. Chem. Soc.* **1968**, *90*, 7364.
(2) Streitwieser, A., Jr.; Muller-Westerhoff, U.; Sonnichsen, G.; Mares, F.; Morrell, D. G.; Hodgson, K. O.; Harmon, C. A. *J. Am. Chem. Soc.* **1973**, *95*, 8644.
(3) Bursten, B. E.; Strittmatter, R. J. *Angew. Chem., Int. Ed. Engl.* **1991**, *30*, 1069.
(4) Evans, W. J.; Forrestal, K. J.; Ziller, J. W. *Angew. Chem., Int. Ed. Engl.* **1997**, *36*, 774.
(5) The term "early actinide metal" is defined herein as Th, Pa, or U.
(6) Billiau, F.; Folcher, G.; Marquet-Ellis, H.; Rigny, P.; Saito, E. *J. Am. Chem. Soc.* **1981**, *103*, 5603.
(7) Eisenberg, D. C.; Streitwieser, A.; Kot, W. K. *Inorg. Chem.* **1990**, *29*, 10.
(8) Boussie, T. R.; Eisenberg, D. C.; Rigsbee, J.; Streitwieser, A., Jr.; Zalkin, A. *Organometallics* **1991**, *10*, 1922 and references therein.
(9) Karraker, D. G.; Stone, J. A. *J. Am. Chem. Soc.* **1974**, *96*, 6885.
(10) Blake, P. C.; Lappert, M. F.; Atwood, J. L.; Zhang, H. M. *J. Chem. Soc., Chem. Commun.* **1986**, 1148.
(11) Edwards, P. G.; Andersen, R. A.; Zalkin, A. *Organometallics* **1984**, *3*, 293.
(12) Dolg, M.; Fulde, P.; Stoll, H.; Preuss, H.; Chang, A.; Pitzer, R. M. *Chem. Phys* **1995**, *195*, 71.
(13) Boeerrigter, P. M.; Baerends, E. J.; Snijders, J. G. *Chem. Phys* **1988**, *122*, 357.
(14) Brennan, J. G.; Green, J. C.; Redfern, C. M. *J. Am. Chem. Soc.* **1989**, *111*, 2373.
(15) Substituents at COT do not significantly affect the e$_{2g}$−e$_{2u}$ separation. See, for example: Rosch, N.; Streitwieser, A., Jr. *J. Organomet. Chem.* **1978**, *145*, 195.
(16) Kaltsoyannis, N.; Bursten, B. E. *J. Organomet. Chem* **1997**, *528*, 19.
(17) Arliguie, T.; Lance, M.; Nierlich, M.; Vigner, J.; Ephritikhine, M. *J. Chem. Soc., Chem. Commun* **1995**, 183.
(18) Li, J.; Bursten, B. E. *J. Am. Chem. Soc.* **1997**, *119*, 9021. Li, J.; Bursten, B. E. *J. Am. Chem. Soc.* **1998**, *120*, 11456.
(19) Gourier, D.; Caurant, D.; Arliguie, T.; Ephritikhine, M. *J. Am. Chem. Soc.* **1998**, *120*, 6084.
(20) King, R. B. *Inorg. Chem.* **1992**, *31*, 1978.

10.1021/ja9903633 CCC: $18.00
Published on Web 07/14/1999

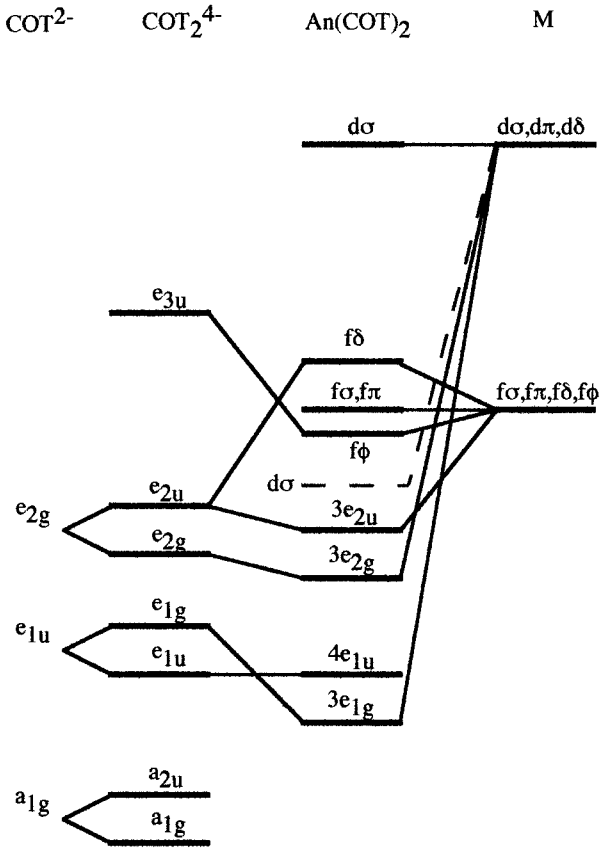

Figure 1. MO diagram for $An(COT)_2$. For $\{Th(COT)_2\}^-$ a nonrelativistic treatment leads to single occupancy of the 5f-based e_{3u} orbital ($f\phi$), wheras inclusion of differential relatavistic effects (dashed lines) leads to single occupancy of the $d\sigma$ ($6dz^2$-based) orbital.

in the figure shows that by incorporating "differential relativistic effects"[12] into the MO calculations, a stabilization of a $6dz^2$ orbital occurs which leads to the placement of this orbital below the 5f series. Now occupation of the lowest unoccupied molecular orbital by one electron gives rise to a $6d^1$ compound that is electronically distinct from $Pa(COT)_2$. The compound $[Th(Cp'')_3]$ ($Cp'' = \eta$-$C_5H_3(SiMe_3)_2$-1,3) is the only known example of a molecule that possesses such a ground state.[22] The possibility of such an electronic configuration for an organoactinide compound was first predicted by Snijders et al.[13] It is interesting to note that additional electrons can also be accommodated in this orbital and in the 5f manifold. The $6dz^2$ orbital is predicted to be virtually nonbonding with respect to the COT ligand group orbitals[16] and so its half-occupation is not expected to either greatly stabilize or destabilize the thorium(III) complex with respect to the parent sandwich compound. Either way, from the MO descriptions, there is nothing wrong on electronic grounds with the concept of a subvalent early actinide metal center stabilized by two COT rings.

Results and Discussion

Use of the bulky, silylated 8-annulene ligand $\{COT(TBS)_2\}^{2-}$ [23] results in the isolation of $[Th\{COT(TBS)_2\}_2]$, **1**,[24] which is an ideal precursor to a thorium(III) sandwich complex. When a slurry of **1** in dimethoxyethane (DME) is stirred over a potassium mirror under argon[25] at room temperature, a gradual color change from yellow to deep green ensues with concomitant dissolution of the starting material; after 24 h, a deep green solution results and ultimately yields deep green prisms of pyrophoric $\{Th[COT(TBS)_2]_2\}K\cdot(DME)_2$ (**2**, see Scheme 1).[26] The complex is virtually insoluble in aliphatic and aromatic hydrocarbons but extremely soluble in tetrahydrofuran (THF) and DME.

Scheme 1

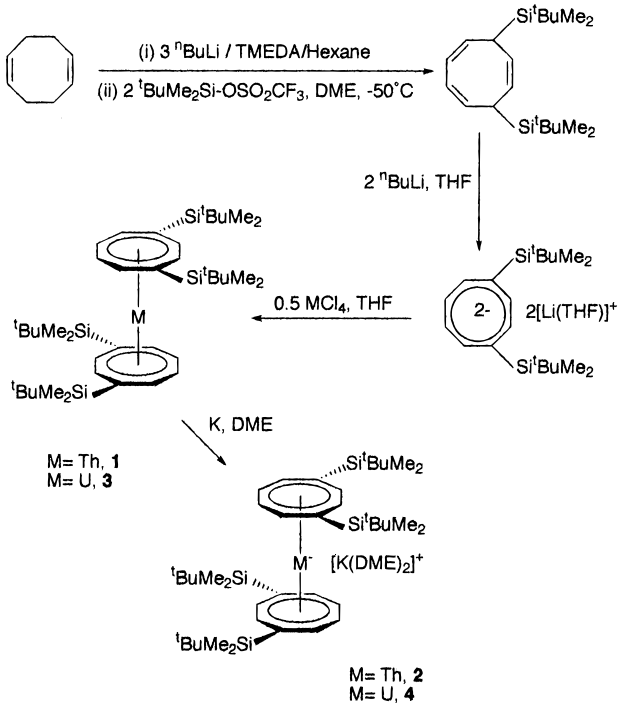

The formulation of **2** as a $6d^1$ compound is supported by the measurement in solution at room temperature of a relatively sharp and intense EPR signal with $g = 1.916$: an electron in a 5f orbital would be expected to relax too quickly to be observed at room temperature.[19,22,27] An EPR signal of a powdered sample of **2** at 298 K (Figure 2a) exhibits a signal typical for an axial or pseudoaxial system with $g_{||} = 1.981$ and $g_{\perp} = 1.887$ with $g_{av} = 1.918$. Superimposed on the latter feature at 110K (Figure 2b) is some fine structure due to hyperfine interactions with the $COT(TBS)_2$ ring protons. The $g_{||}$ value is close to 2 because an electron in the dz^2 orbital cannot orbit about the z axis and so the z component of the orbital angular momentum is quenched, but spin−orbit coupling can cause mixing with the dxz and dyz orbitals, lowering the value of $g_{\perp}$. Similar features are displayed by the 17-electron sandwich complex [Zr(η-COT)(η-C_5Me_5)], where the odd electron resides in a $4dz^2$ orbital.[28]

The magnetic moment (uncorrected) of **2**, measured as a d_8-tetrahydrofuran (thf) solution by the Evans method, is 1.20 μ_B

(21) The π-acceptor properties of silyl substituents on arene rings are well documented, for example see: Jia, L.; Yang, X.; Stern, C. L.; Marks, T. J. *Organometallics* **1997**, *16*, 842 and references therein.

(22) Kot, W. K.; Shalimoff, G. V.; Edelstein, N. M.; Lappert, M. F. *J. Am. Chem. Soc.* **1988**, *110*, 986. Bursten, B. E.; Rhodes, L. F.; Stritmatter, R. J. *J. Am. Chem. Soc.* **1989**, *111*, 2756.

(23) This ligand was prepared by a modification to the route for the 1,4-bis(trimethylsilyl)cycloocta-1,3,5-triene. See Experimental Section.

(24) See Experimental Section.

(25) Argon impurities rated to <0.5 ppm.

(26) The nature of the coordinated ether is important. When the reaction is performed in THF or 18-crown-6 is added to the product from DME, only green oils are isolated.

(27) A classical explanation for this, treating the electron as a standing wave, is that f-orbitals have more angular nodes than d orbitals and hence a shorter wavelength. By the deBroglie relationship, $\rho = 1/\lambda$, hence f orbitals have a greater orbital angular momentum than d orbitals, increasing the magnitude of the spin−orbit coupling constant. This leads to faster electronic relaxation by spin−orbit coupling mechanisms.

(28) Gourier, D.; Samuel, E.; Teuben, J. H. *Inorg. Chem.* **1989**, *28*, 4663.

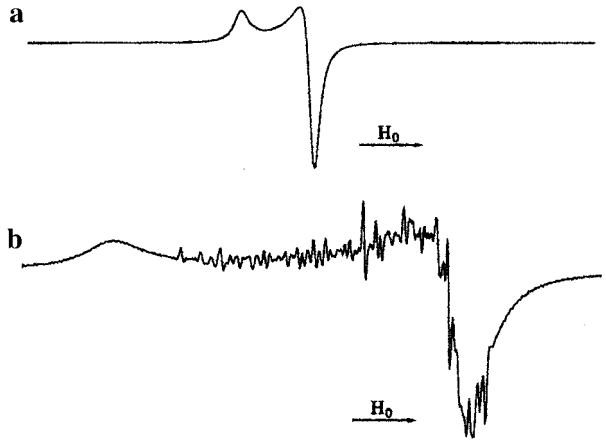

Figure 2. 2. (a) EPR spectrum of a powdered sample of **2** at 298 K. (b) EPR spectrum of a powdered sample of **2** at 110 K.

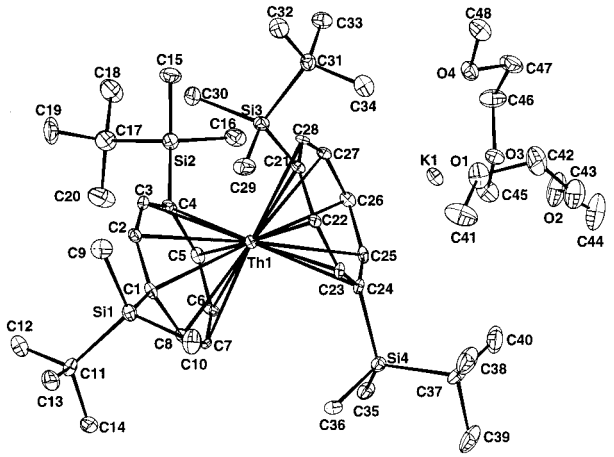

Figure 3. ORTEP[33] view of $\{Th[COT(TBS)_2]_2\}K\cdot(DME)_2$ **2** (thermal ellipsoids at 50%).

at 293 K, and is low when compared to the spin-only value for one unpaired electron (1.73 μ_B). The most obvious reason for this, given the highly reactive nature of the compound, is contamination by oxidation products such as [Th{COT-(TBS)$_2$}$_2$]. However, there is no evidence by ^{1}H NMR spectroscopy of any such diamagnetic contamination. Resonances are seen, however, that are due to DME displaced from the potassium centers by the NMR solvent (d_8-thf) and a broad paramagnetic signal due to the ligand *tert*-butyl units. Rather, we think that the low magnetic moment is due to mixing of the ground-state magnetic component with low-lying excited states. This is supported by remeasurement of the moment at 199 K, which yields a value of 1.41 μ_B. UV−visible spectroscopy identifies two broad and intense bands at 705 and 826 nm, presumably due to allowed (and hence intense) 6d to 5f electronic transitions that are responsible for the green color of the compound. Of great interest would be the lowest energy transition in this series: this is expected to come in the near-infrared region of the electromagnetic spectrum, as it is predicted to do so in [ThCp″$_3$].[16] Unfortunately, a scan to 2500 nm proved inconclusive. The 5f based levels (Figure 1) will be further split by spin−orbit coupling, so that detailed assignment of the observed transitions is not realistic; however, their intensity is in accord with a 6d^1 ground state, i.e. single occupation of the dσ level (dotted line in Figure 1), for **2**; in contrast, the UV−visible spectrum of the analogous U(III) complex **4** displays only a series of weak (forbidden) f−f transitions.

The structure of **2** is presented in Figure 3, with selected bond lengths and angles and data collection parameters detailed in Tables 1 and 2, respectively.

The ring centroid−metal−ring centroid angle, cen−M−cen, deviates from linearity by approximately 5°; this structural motif has been observed in several COT complexes before, and has been postulated to arise from intramolecular forces such as van der Waals attractions.[8] Interestingly, all the *tert*-butyl groups point away from the metal, presumably to alleviate unfavorable inter-ring steric interactions, although no restricted rotation about the ring carbon−silicon bond is evident on the NMR time scale in solution for the uranium analogue (vide infra),[29] indicating that, barring a very high energy barrier to rotation, these groups do project across the inter-ring space in solution and provide steric protection to the metal center. One of the coordinated ether units exhibits an asymmetry in metal−oxygen bond lengths with one very long bond to K (the "normal" K−O bond lengths range from 2.655(5) to 2.764(4) Å, whereas the abnormal bond, K(1)−O(2), is 2.898(5) Å). This suggests that one chelating ether unit may be labile. In fact, samples crystallized from pure DME tend to collapse to powders when the last traces of solvent are removed in vacuo.

(29) A plot of δ vs 1/T from −80 to +70 °C for the *t*BuSi and Me_2Si groups is linear.

Table 1. Selected Bondlengths (Å) and Angles (deg) for **2** and **4**

	M = Th	M = U		M = Th	M = U
M(1)−C(1)	2.796(6)	2.732(5)	M(1)−C(21)	2.842(6)	2.783(5)
M(1)−C(2)	2.780(6)	2.709(5)	M(1)−C(22)	2.803(6)	2.775(5)
M(1)−C(3)	2.746(6)	2.702(5)	M(1)−C(23)	2.797(6)	2.753(5)
M(1)−C(4)	2.773(6)	2.742(5)	M(1)−C(24)	2.783(6)	2.761(5)
M(1)−C(5)	2.756(6)	2.717(5)	M(1)−C(25)	2.775(6)	2.732(5)
M(1)−C(6)	2.792(6)	2.745(5)	M(1)−C(26)	2.755(6)	2.731(5)
M(1)−C(7)	2.781(6)	2.717(5)	M(1)−C(27)	2.771(6)	2.758(5)
M(1)−C(8)	2.747(6)	2.696(5)	M(1)−C(28)	2.782(6)	2.742(5)
M(1)−Cen(1)	2.067	1.998	M(1)−Cen(2)	2.094	2.042

	M = Th	M = U
Cen(1)−C(1)−Si(1)	177.6	178.2
Cen(1)−C(4)−Si(2)	175.0	177.2
Cen(2)−C(21)−Si(3)	177.3	178.1
Cen(2)−C(24)−Si(4)	174.2	175.1

Table 2. Crystal Data and Structure Refinement for **2** and 4

	2	**4**
diffractometer	Enraf Nonius fitted with FAST-TV area detector processed by MADNESS software	
empirical formula	$C_{48}H_{92}KO_4Si_4Th$	$C_{48}H_{92}KO_4Si_4U$
formula weight	1116.72	1122.71
temp, K	120(2)	120(2)
wavelength, Å	0.71069	0.71069
crystal system	orthorhombic	orthorhombic
space group	Pbcn	Pbcn
unit cell dimensions		
a, Å	19.0274(14)	19.1026(5)
b, Å	26.419(4)	26.493(5)
c, Å	23.9502(12)	23.701(4)
volume, Å^3	12040(2)	11995(3)
Z	8	8
density(calcd), Mg/mÅ^3	1.232	1.243
F(000)	4616	4632
crystal color	green	deep orange
crystal size, mm	0.28 × 0.145 × 0.145	0.35 × 0.18 × 0.18
meta range for data collection, deg	1.76−25.08	1.76−25.081
goodness-of-fit on F^2	0.725	0.882
final *R* indices [$I > 2\sigma(I)$]	R1 = 0.0310, wR2 = 0.0733	R1 = 0.0302, wR2 = 0.0747
R indices (all data)	R1 = 0.0777, wR2 = 0.1324	R1 = 0.0553, wR2 = 0.1212

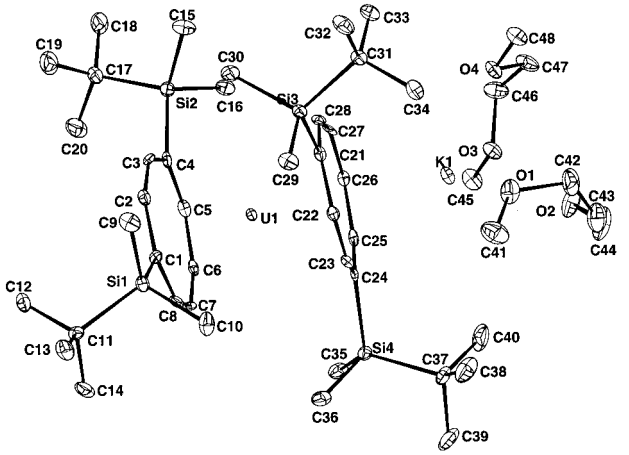

Figure 4. ORTEP[33] view of {U[COT(TBS)$_2$]$_2$}K·(DME)$_2$ **4** (thermal ellipsoids at 50%).

Comparison with isostructural {U[COT(TBS)$_2$]$_2$}K·(DME)$_2$, **4**, made similarly from U[COT(TBS)$_2$]$_2$ (**3**) and potassium (see Scheme 1), affords the first opportunity to contrast the metrical parameters of trivalent thorium, trivalent uranium, and tetravalent thorium where each metal center possesses an identical ligand environment.[31] The structure of **4** is presented in Figure 4, with selected bond lengths and angles and data collection parameters detailed in Tables 1 and 2, respectively.

For both anionic complexes, the M−C distances for the ring capped by K (M−C(ring 2)) are on average longer than those for the uncapped ring (M−C(ring 1)): U−C(ring 1) 2.720(5) Å, U−C(ring 2) 2.753(5) Å; Th−C(ring 1) 2.771(6) Å, and Th−C(ring 2), 2.789(6) Å. This trend is also reflected in the metal−centroid (M−cen) distances: U−cen 1, 1.998 Å, U−cen 2, 2.042 Å; Th−cen 1, 2.066 Å, Th−cen 2, 2.090 Å. This effect has been noticed before and ascribed to the electrostatic influence of the alkali metal ion.[8] The average Th(III)−C(Ring) distance is 2.780 Å, and the corresponding U(III)−C(ring) distance is 2.737(5) Å. The average Th(IV)−C(ring) and Th(IV)−cen distances in [Th(COT(TBS)$_2$)$_2$] (see Supporting Information) are 2.718 and 1.999(7) Å, respectively, implying that the metal radius in the Th(III) compound is approximately 0.04 and 0.06 Å larger than the radii in the U(III) and Th(IV) compounds, respectively. As mentioned above, the cen−M−cen angles all deviate slightly from linearity (174.5°, 172.4°, 172.3°; Th(III), U(III), Th(IV), respectively) and the silyl groups bend in slightly toward the metal center, the cen−C(ring)−TBS angle ranging from approximately 174 to 178° for all three compounds.

Conclusions

We have shown that silylated COT ligands can stabilize low oxidation state early actinide metal centers in sandwich complexes both thermodynamically (by virtue of metal−ring orbital interactions) and kinetically (by virtue of bulky ligand substituents).

Experimental Section

General Comments. All air-sensitive materials were manipulated under dry nitrogen in a drybox or by standard high-vacuum and Schlenk techniques. The synthesis and manipulation of compounds **2** and **4** required argon rated to <0.5 ppm impurities. NMR solvents were dried over molten K and vacuum distilled. Microanalyses were by Mikroanalytisches Labor Pascher, Remagen-Bandorf, Germany. Cyclooctadiene and *t*-BuSiMe$_2$SO$_3$CF$_3$ were purchased from The Aldrich Chemical Co., Ltd. ThCl$_4$ was synthesized by passing N$_2$-containing CCl$_4$ vapor over ThO$_2$ in a quartz boat at 750 °C inside a quartz tube, causing the product to sublime out as white crystals. UCl$_4$ was prepared by the literature procedure.[30]

X-ray Crystallographic Study on 2. Crystals suitable for X-ray diffraction were grown by diffusion of pentane into concentrated DME solutions at room temperature and were coated in oil before mounting on the diffractometer at 120 K.

5,8-Bis(*t*BuSiMe$_2$)cycloocta-1,3,6-triene. 1,5-Cyclooctadiene (16.9 mL, 0.138 mol) was treated with 3 equiv of *n*BuLi (166 mL of a 2.5 M solution, 0.415 mol) and 3 equiv of tetramethylethylenediamine (TMEDA) (62.5 mL, 0.415 mol), as in the synthesis of trimethylsilyl-COT derivatives.[32] The volatiles were removed in vacuo and the residue extracted with dimethoxyethane (DME) (600 mL). This was filtered through Celite on a glass sinter to remove LiH. The Celite was washed with an additional aliquot of DME (200 mL) and the filtrates combined. This deep red DME solution was then cooled (−50 °C) in a cold bath leading to precipitation of a pale green solid. To this suspension was added dropwise neat *t*BuMe$_2$SiSO$_3$CF$_3$ (63.2 mL, 72.7 g, 0.275 mol), with stirring. An exothermic reaction ensued and the reaction mixture was maintained at −40 °C with additional cooling. Close to the end of the addition, the solid disappeared leaving a clear pale yellow solution. This was allowed to warm to room temperature and stirred for 3 h. The solvent was then removed in vacuo with the aid of a hot water bath (70 °C). The resulting mixture of oil and crystalline LiSiSO$_3$CF$_3$ was extracted with petroleum ether (300 + 100 mL) and filtered via cannula. The solvent was removed from the filtrate in vacuo to leave a yellow oil, 5,8-bis(*t*BuSiMe$_2$)cycloocta-1,3,6-triene, that was greater than 95% pure by ^{1}H NMR spectroscopy. Yield 29.3 g, 0.088 mol, 64% based on COD. ^{1}H NMR (CDCl$_3$, 300 MHz, +20 °C): δ −0.02 (s, 12H, Si*Me*$_2$), δ 0.88 (s, 18H, Si*CMe*$_3$), δ 2.93 (m, 2H, −*CH*$_2$), δ 5.47 (d, J = 1 Hz, 2H, −*CH*$_2$), δ 5.54 (t, J = 9.5 Hz, 2H, −*CH*$_2$), δ 5.78 (m, 2H, −*CH*$_2$). *m*/*e* 334 (M$^+$).

Li$_2$[1,4-bis(*t*BuSiMe$_2$)COT]·THF. To a cooled solution of 5,8-bis(*t*BuSiMe$_2$)cycloocta-1,3,6-triene (22.6 g, 0.068 mol, 0 °C) was added slowly by syringe 2 equiv of 2.5M *n*BuLi solution in hexanes (54.5 mL, 0.136 mol). The solution was allowed to warm to room temperature and was then stirred for 1 h. The solvents were removed in vacuo and the gummy solid placed in a hot water bath under dynamic vacuum (30 min, 70 °C). The resulting brittle solid was broken up into small pieces with a spatula and washed with cold pentane (−50 °C, 2 × 80 mL) and then returned to the water bath as before for an additional 1 h. This procedure afforded a gray solid, Li$_2$[1,4-bis(*t*BuSiMe$_2$)COT]·THF, that was consistently shown to contain one molecule of THF per dianion by ^{1}H NMR spectroscopy. Yield 19.55 g, 0.047 mol, 69%). ^{1}H NMR (C$_6$D$_6$, 300 MHz, +20 °C): δ 0.74 (m, 4H, O-*CH*$_2$CH$_2$), δ 0.87 (s, 12H, Si*Me*$_2$), δ 0.88 (s, 18H, Si*CMe*$_3$), δ 2.47 (m, 4H, O-CH$_2$*CH*$_2$), δ 6.19 (s, 2H, −C*H*), δ 6.27 (s, 2H, −*CH*), δ 6.40 (s, 2H, −*CH*).

[Th{COT(TBS)$_2$}$_2$] (1). To a suspension of sublimed ThCl$_4$ (1.35 g, 3.61 mmol) in cold THF (20 mL, −70 °C) was added a solution of Li$_2$[1,4-bis(*t*BuSiMe$_2$)COT]·THF (3.00 g, 7.22 mmol) in cold THF (30 mL, −70 °C). The mixture was allowed to warm to room temperature and stirred for 20 h, during which time it turned yellow. The solvent was removed in vacuo and the product extracted with toluene (100 mL) and filtered. The solvent was removed and the solid washed with pentane (2 × 20 mL) and dried in vacuo, yielding **1** as a yellow powder (2.20 g, 2.46 mmol, 68%). ^{1}H NMR (C$_6$D$_6$, 300 MHz, +20 °C): δ 0.73 (s, 18H, Si*CMe*$_3$), δ 0.77 (s, 6H, Si*Me*$_2$), δ 0.67 (s, 6H, Si*Me*$_2$), δ 6.77 (m, 2H, ring-*CH*), δ 6.86 (m, 4H, ring-*CH*). Anal. Calcd for C$_{40}$H$_{72}$Si$_4$Th: C, 53.54; H, 8.09. Found: C, 54.02; H, 8.44. *m*/*e* 897 (M$^+$).

(30) Hermann, J. A.; Suttle, J. F.; Hoekstra, H. R. *Inorg. Synth.* **1974**, *15*, 243.

(31) The only other example where an analogous comparison is possible is between Th(Cp″)$_3$ and U(Cp″)$_3$. Unfortunately, the crystal structure of the latter has not been published. See: Lukens, W. W.; Blosch, L. L.; Andersen, R. A. *J. Am. Chem. Soc.* **1996**, *118*, 901. Blake, P. C.; Lappert, M. F.; Atwood, J. L.; Zhang, H. M. *J. Chem. Soc., Chem. Commun.* **1986**, 1148.

(32) Burton, N.; Cloke, F. G. N.; Joseph, S. C. P.; Karamallakis, H.; Sameh, A. A. *J. Organomet. Chem* **1993**, *462*, 39.

(33) Johnson, C. K. ORTEP II, Report ORNL-5738, Oak Ridge National Laboratory, Tennessee, 1976.

{**Th[COT(TBS)$_2$]$_2$}K·(DME)$_2$ (2).** A suspension of **1** (2.00 g, 2.23 mmol) in DME (50 mL) was added to a K mirror (0.40 g, 0.01 mol, 4.5 equiv). The mixture immediately began to change color and within $^1/_2$ h was deep green. This was stirred for 48 h to give a clear deep green solution that was filtered from the excess K and concentrated to ca. 10 mL. Cooling (−50 °C, 5 days) afforded large green prisms of **2** which were isolated by decantation and dried in vacuo. The supernatant was triturated with pentane (40 mL) causing the crystallization of copious amounts of **2** and decolorization of the solution. The solid was isolated by filtration and dried in vacuo to yield a second crop of **2**. The crops were combined and washed with toluene (3 × 10 mL), dried in vacuo, and then redissolved in a minimum amount of DME (ca. 15 mL) with rapid stirring. The stirring was stopped and pentane slowly added (ca. 20 mL) causing the crystallization of **2** as small iridescent green prisms, which were isolated by filtration and dried in vacuo (1.60 g, 1.56 mmol, 70%). Anal. Calcd for $C_{48}H_{92}KO_4Si_4Th$: C, 51.63; H, 8.30. Found: C, 50.32; H, 8.27. The low C analysis is presumably due to thorium carbide formation.

[U{COT(TBS)$_2$}$_2$] (3) was obtained from UCl_4 (1.02 g, 2.68 mmol) and Li_2(COT(TBS)$_2$)·THF (2.20 g, 5.26 mmol) as a deep green powder (1.86 g, 2.06 mmol, 78%). Solutions of **2** are green/red dichroic. ^{1}H NMR ($C_6D_5CD_3$, 300 MHz, +20 °C): δ +6.7 (s, 18H, Si*CMe*$_3$), δ −16.7 (s, 6H, Si*Me*$_2$), δ −21.2 (s, 6H, Si*Me*$_2$), δ −23.2 (s, 2H, −*CH*), δ -41.6 (s, 2H, −*CH*), δ −48.2 (s, 2H, −*CH*). $\Delta\nu_{1/2}$ ranges between 10 and 30 Hz. Anal. Calcd for $C_{40}H_{72}Si_4U$: C, 53.18; H, 8.03. Found: C, 53.57; H, 8.22. *m*/*e* 903 (M^+).

{**U[COT(TBS)$_2$]$_2$}K·(DME)$_2$ (4)**. **4** was prepared analogously to **2** from **3** (1.86 g, 2.06 mmol) and K (0.40 g, 0.01 mol, 4.9 equiv) in DME, yielding small iridescent deep orange needles on trituration of deep red DME solutions with pentane (1.61 g, 1.58 mmol, 77%). ^{1}H NMR (C_4D_8O, 300 MHz, +22 °C): δ +2.36, $\Delta\nu_{1/2=33\ Hz}$ (18H); δ −16.51, $\Delta\nu_{1/2=95\ Hz}$ (6H); δ −8.00, $\Delta\nu_{1/2=135\ Hz}$ (6H); δ −24.1, $\Delta\nu_{1/2=413\ Hz}$ (2H); δ −30.4, $\Delta\nu_{1/2=410\ Hz}$ (2H); δ −37.6, $\Delta\nu_{1/2=402\ Hz}$ (2H). Anal. Calcd for $C_{48}H_{92}KO_4Si_4U$: C, 51.35; H, 8.26. Found: C, 51.60; H, 8.38.

Acknowledgment. We thank the EPSRC for a Postdoctoral Fellowship (J.P.) and P. Roussel, A. Hughes, and P. Scott for technical assistance and the near-IR data.

Supporting Information Available: Tables of X-ray data for **1**, **2**, and **4** (PDF). This material is available free of charge via the Internet at http://pubs.acs.org.

JA9903633